

Principles of laser-induced separation and transport of living cells

Verena Horneffer*

Norbert Linz

Alfred Vogel

University of Lübeck
Institute of Biomedical Optics
Peter-Monnik Weg 4
D-23562 Lübeck, Germany
E-mail: vogel@bmo.uni-luebeck.de

Abstract. Separation and transport of defined populations of living cells grown on a thin membrane can be achieved by laser microdissection (LMD) of the sample of interest, followed by a laser-induced forward transport process [laser pressure “catapulting” (LPC)] of the dissected cell cluster. We investigate the dynamics of LMD and LPC with focused and defocused UV-A laser pulses by means of time-resolved photography. Catapulting is driven by plasma formation when tightly focused pulses are used, and by confined thermal ablation at the bottom of the sample for defocused catapulting. With both modalities, the initial specimen velocity amounts to about 50 to 60 m/s. Time-resolved photography of live cell catapulting reveals that in defocused catapulting, strong shear forces arise when the sample is accelerated out of the culture medium covering the cells. By contrast, pulses focused at the periphery of the specimen cause a fast rotational movement that minimizes the flow of culture medium parallel to the sample surface, and thus the resulting shear stresses. Therefore, the recultivation rate of catapulted cells is much higher when focused pulses are used. Compared to collateral damage by mechanical forces, side effects by heat and UV exposure of the cells play only a minor role. © 2007 Society of Photo-Optical Instrumentation Engineers. [DOI: 10.1117/1.2799194]

Keywords: laser microdissection; laser pressure catapulting; time-resolved photography; cell transport; cell separation.

Paper 07059R received Feb. 23, 2007; revised manuscript received May 29, 2007; accepted for publication Jun. 1, 2007; published online Oct. 29, 2007.

1 Introduction

Procurement of well-defined small samples of histologic material for proteomic and genomic analysis has become important with the increasing refinement of analytic techniques. Furthermore, separation and transport of living cells is of interest for stem cell research, organ culture, and tissue engineering. Mechanical separation techniques are tedious, time consuming, and bear the risk of contamination. Therefore, faster laser-based processes have been developed.^{1–3} A widespread, rapid, contact- and contamination-free separation method consists in laser microdissection (LMD) of the sample of interest, and subsequent laser-induced forward transport of the dissected material into a vial, which is used for further analysis.^{4–6} For the transport process, the expression “laser pressure catapulting” (LPC) has been coined, and the combined separation and procurement procedure is often termed LMPC. The sample is usually placed on a thin, UV-absorbing polymer foil that is mounted on a routine microscope glass slide or into a transparent culture dish. A region of interest is separated from the sample using a sequence of focused UV-A

laser pulses, and subsequently catapulted into the cap of a microfuge tube by a final, typically more energetic, laser pulse.

The LMPC technique has first been applied for the procurement of histologic material.^{4–6} However, recently a protocol for life cell catapulting and recultivation has been developed^{7,8} that extends its possibilities into the fields of stem cell research and tissue engineering without changing the cells.^{9,10} The protocol is designed to handle adherent cells growing on a polymer membrane in a culture dish and makes it possible to separate specific cell types or clusters out of a heterogeneous cell population. Cell separation is thus inherently a two-step procedure, with identification and dissection of the cells of interest preceding the transport step and recultivation.

Alternative approaches are matrix-assisted pulsed laser evaporation direct write (MAPLE-DW) of cells,^{11,12} biological laser printing (BioLP),¹³ and absorbing-film-assisted laser-induced forward transfer (AFA-LIFT).^{14,15} These approaches are all geared toward the transfer of cells out of a homogeneous reservoir for purposes of tissue engineering. The reservoir consists either of cells grown on matrigel^{11,12} or of cells suspended in a liquid growth medium.^{13–15} Since the reservoir is homogeneous, no dissection step is required before transfer. Cells are transported together with the medium (gel or liquid)

Address all correspondence to Alfred Vogel, Institute of Biomedical Optics, University of Lübeck, Peter-Monnik-Weg 4, D-23562 Lübeck, Germany. Tel: 49 451 500 6504; Fax: 49 451 500 6546; E-mail: vogel@bmo.uni-luebeck.de

*Current affiliation: London Metropolitan University, Institute of Brain Chemistry and Human Nutrition, 166-220 Holloway Road, N7 8DB London, United Kingdom.

into which they are embedded, and the irradiated area of the reservoir layer is separated from the surrounding regions merely by the laser-induced acceleration.

It is the goal of the present study to elucidate the mechanisms and potential side effects of LMPC of living cells to find the most efficient and gentle transfer strategy. In MAPLE-DW, BioLP, or AFA-LIFT, cohesion of the transported volume is often lost during the transport process. By contrast, in LMPC, usually a relatively large cluster of adherent cells is catapulted as one entity together with the supporting membrane that serves to maintain the mechanical integrity of the specimen during the transport process. This approach allows the use of either focused or defocused laser pulses to drive catapulting. In the original protocol developed by Mayer et al.⁷ and Stich et al.,⁸ pulses focused at the periphery of the dissected specimen are employed. We observed in a previous study of laser-induced transport of histologic specimens that focused catapulting relies on plasma formation at the bottom of the sample, which is accompanied by a dramatic pressure rise that drives catapulting and, as a collateral effect, produces a hole in the specimen.¹⁶ When the plasma is generated at the specimen's periphery, the inhomogeneous distribution of pressure results in an oblique flight direction. In the same study, catapulting was found to be driven by photothermal ablation when a defocused laser beam irradiating a spot more than 25 μm diam was used. This approach was associated with absence of hole formation, a stable flight trajectory when the pulses were aimed at the center of the specimen, and by moderate catapulting velocities when spot sizes comparable to the specimen diameter and small radiant exposures were used. Since these features seem to be beneficial for the laser-based transport of live cells, this technique is tested in the present study and compared with the success rate of the original protocol. The mechanisms of live cell catapulting are, for both catapulting modalities, investigated by time-resolved photography, and the success of LMPC is measured by the transfer and recultivation rates. Mechanical side effects are assessed by evaluating the high-speed photographic image series. Potential thermal and UV-light-induced side effects are discussed based on the optical and thermal properties of the cells and the supporting materials that were determined previously.¹⁶

2 Materials and Methods

2.1 Apparatus for Microdissection and Laser-Induced Transport

We used a microbeam system equipped with an N_2 laser ($\lambda = 337$ nm) emitting pulses of 3-ns [full width half maximum (FWHM)] duration (Palm Microlaser Technologies, Bernried, Germany). The laser beam is coupled into an inverted microscope (Axiovert 200, Carl Zeiss MicroImaging GmbH, Goettingen, Germany) with a motorized, computer-controlled stage. The microscope objective used in this study was a Zeiss LD Plan Neofluar $20\times/0.5$. An energy calibration showed that the relation between the setting at the laser control unit and the actual energy transmitted through the objective is logarithmic.

The focal spot diameter ($1/e^2$ irradiance values) as determined by a knife-edge measurement was 21 μm , much larger than the diffraction-limited focus diameter of 0.82 μm . Nev-

ertheless, holes with 4 to 5 μm could be created in the polyethylene naphthalate (PEN) foil, and the cutting width in PEN foil was about 6 μm . These observations can be explained by the fact that the irregular N_2 laser beam profile results in a focal irradiance distribution featuring a broad base and a central hot spot (Fig. 3 of Ref. 16). Part of the spot size enlargement is, furthermore, due to the fact that the laser beam is coupled into the light path for fluorescence illumination, which is optimized for creating a homogeneous illumination of the object plane but not for focusing a laser beam.

2.2 Cultivation, Laser-Mediated Separation, and Recultivation of Cells

For the cultivation and retrieval of live cells by LMPC, we used either duplex membrane dishes (Palm Microlaser Technologies, Bernried, Germany)⁷ or the combination of a membrane ring (Palm Microlaser Technologies, Bernried, Germany) lying in a Lumox dish (Greiner BIO-One, Frickenhausen, Germany).^{7,8} In both cases, a 25- μm -thick gas-permeable Teflon foil (Dupont Teijin Films, Luxembourg) provides mechanical support, and a 1.35- μm -thick UV-absorbing polymer foil (polyethylene naphthalate, PEN, Dupont Teijin Films, Luxembourg) is mounted into the dish above the Teflon foil, as delineated in the insert of Fig. 1. The top of the PEN foil was conditioned with 0.1-mg/mL polylysine solution (MG >300,000, Biochrom, Berlin, Germany). After removal of the polylysine solution, Chinese hamster ovary (CHO) cells were cultivated on this foil in a humidified incubator (37°C , 5% CO_2) until a confluent monolayer was grown. Ham's F12 enriched with 10% fetal bovine serum and 1% antibiotic/antimycotic solution (all supplied by PAA Laboratories, Cölbe, Germany) was used as medium. To compensate for evaporation losses, 100- μL buffer solution was added into the membrane dish every 10 min once it had been placed under the microscope. Some experiments were done without any fluid between Teflon membrane and PEN foil, but usually some liquid enters the space between the two membranes during dissection. Since we observed that the presence of this liquid enhanced the catapulting, in most experiments a well-defined amount of medium was injected between the membranes before LMPC. The resulting liquid layer had a thickness of 30 to 100 μm .

Before LMPC, the culture medium was almost completely removed such that only a thin layer of liquid [10 to 50 μm thick, as determined by optical coherence tomography (OCT)] remained above the cells. Then the region of interest was dissected, and the dissectat (cells and PEN foil) was catapulted by a single laser pulse into the cap of a microfuge tube that had been wetted with culture medium. The original protocol involves the use of focused laser pulses for catapulting, but we also performed series of experiments with defocused pulses, because we hoped that this would minimize bending of the specimen and shear stresses on the cells. For recultivation after LMPC, the cells were transferred from the microfuge cap into 12 well plates, as described by Stich et al.,⁸ and grown under the same condition as the original culture.

With both catapulting modalities, usually 1- μJ pulses were used for dissection and 12- μJ pulses for catapulting. Only in exceptional cases, when the liquid layer between Teflon foil and PEN foil was very thick, up to 5- μJ pulse energy was

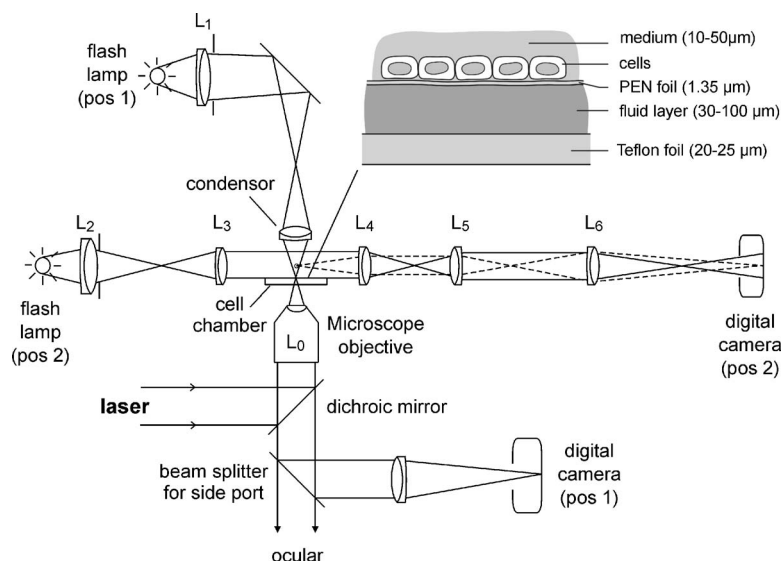


Fig. 1 Setup for time-resolved investigations of the dynamics of laser-induced transport of live cells in a microbeam apparatus. The insert shows a detailed view of the chamber used for cultivation and subsequent separation of a defined population of living cells. Cells are grown on a 1.35- μm -thick PEN foil supported by a 25- μm -thick Teflon foil, and are covered by culture medium. A liquid layer of variable thickness (30 to 100 μm) separates the two foils. For separation, the desired cell population is first, together with the PEN foil supporting the cells, severed from their surroundings by microdissection using laser pulses focused through L_0 . The culture medium is then almost completely removed, such that only a thin layer of liquid remains above the cells (10 to 50 μm). Finally, the dissectat is catapulted into a cap of a microfuge tube placed closely above the culture dish. The dissection step was photographed in a top view and the catapulting step in a side view, both with 18-ns time resolution.

used for dissection. The catapulting energy was selected as low as possible to achieve reproducible material transport in spite of the variations of the liquid layer covering the cells.

2.3 Optical and Thermal Material Parameters

Table 1¹⁷⁻²³ presents a summary of the optical and thermal properties of materials relevant for LMD and LPC of living cells. The transmission properties of CHO cells were determined by measurements in the microbeam setup at low irradiance values, for which nonlinear absorption is negligible.

For the determination of the optical properties of the PEN foil, we used an integrating sphere, since PEN both absorbs and scatters strongly at $\lambda=337$ nm. The heat capacity of the PEN foil was determined by differential scanning calorimetry, and the phase transition temperature of PEN (corresponding to its photothermal dissociation temperature) was obtained through thermogravimetric analysis. Details of the experimental procedures are described in Ref. 16. The other data listed in Table 1 were taken from the literature, with the sources listed in the table caption.

Table 1 Optical properties at 337 nm and thermal properties of cells, polyethylene naphthalate (PEN) polymer foil, Teflon foil, and water. All transmission data are corrected for specular reflection, i.e., they represent purely the transmission of the sample. The data for water absorption were taken from the literature,¹⁷ as well as the data for heat conductivity, heat capacity, and density of water and PEN.^{18,19} The “phase transition temperature” corresponds for PEN to the temperature at which photothermal dissociation into gaseous components occurs, for water to the superheat limit in bubble-free liquid water,²⁰ and for cells to their heterogeneous nucleation threshold,^{21,22} above which the cell is destroyed by vapor bubble formation around nucleation centers within the cell. Due to the short heat exposure time, bubble formation rather than thermal denaturation construes the damage threshold for cells.^{22,30}

Material	Sample thickness x (μm)	Transmission (%)	Extinction coefficient μ_{eff} (cm^{-1})	Optical penetration depth δ (μm)	Average heat capacity ($\text{kJ K}^{-1} \text{kg}^{-1}$)	Phase transition temperature ($^{\circ}\text{C}$)	Heat conductivity ($\text{W m}^{-1} \text{K}^{-1}$)	Density (kg m^{-3})
PEN foll	1.35	$I=20.5$ $R=22.4$	$\mu_a=3520$ $\mu_s=8680$ $\mu_{\text{eff}}=11360$	0.88	2.7	460	≈ 0.4	1.39
Teflon foll	≈ 25	95.8	17.2	580	1.0	—	≈ 0.2	2200
CHO cells	≈ 5	93.8	127	79	4.0	150 to 300		≈ 1000
Water			0.0172	5.8×10^5	4.187	300	0.598	998

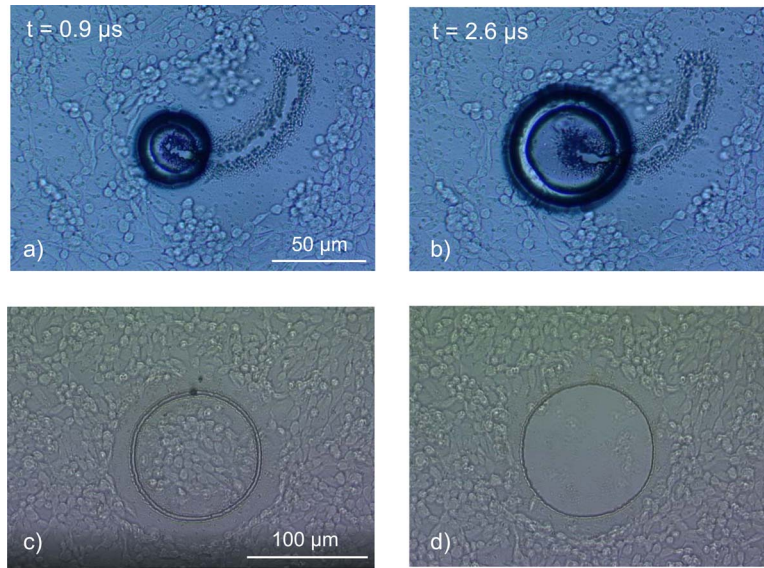


Fig. 2 Laser dissection and catapulting of CHO cells with relatively low adhesion to the PEN foil. In (a) and (b), the cavitation bubble dynamics during dissection of CHO cells are shown at different times, with (b) being the stage of maximum expansion. (c) and (d) show the target sample after dissection and catapulting, respectively. We used a $20\times$ objective, $NA=0.5$. The laser pulse energies used for dissection were $E=5\ \mu\text{J}$ in (a) and (b), and $E=1.0\ \mu\text{J}$ in (c) and (d).

2.4 Time-Resolved Photography of Dissection and Catapulting

The mechanisms of dissection and catapulting of living cells were analyzed by time-resolved photography using the experimental setup of Fig. 1. The dynamics were investigated with a temporal resolution better than 100 ns by taking series of single frame photographs with increasing time delay between catapulting laser pulse and the instant at which the photograph was exposed. The N_2 laser pulses for dissection and catapulting were focused through the microscope objective L_0 into the cell chamber containing the specimen of interest.

For time-resolved photography of the dissection process, we replaced the halogen lamp of the microscope by a plasma discharge lamp with 18-ns duration (Nanolite KL-L, High-Speed Photo-Systeme, Wedel, Germany, mounted at position 1). The collimation optics of the halogen lamp was substituted by a Nikon $f=50\ \text{mm}$, $F=1.2$ objective (L_1) connected to the flash lamp. The free-running mode of the flash lamp at 20-Hz repetition rate was used for alignment and focusing purposes, and single externally triggered pulses were used to obtain the photographs. The dissection dynamics were imaged through the microscope optics (L_0) onto the chip of a 6-megapixel digital camera (FinePix S1 Pro, Fujifilm, Sendai, Japan) attached to a side port of the microscope (position 1). Appropriate trigger and delay electronics enabled us to adjust the time between catapulting laser pulse and flash lamp discharge with the precision of a few nanoseconds.

To document the catapulting dynamics, the specimen was imaged in transillumination in side view using the light of the 18-ns Nanolite flash lamp mounted at position 2. We used Koehler-type illumination optics consisting of an $f=50\ \text{mm}$, $F=1.2$ collimator (L_2) and an $f=250\ \text{mm}$, $F=6.2$ condenser (L_3). The long focal length of the condenser provided the large working distance required because of the large width of

the microscope stage. The specimens were imaged using a $10\times$, $NA=0.28$ objective (L_4) with 33.5-mm working distance (M Plan Apo, Mitutoyo Corporation, Kawasaki, Japan), and a tube lens (L_5) with 200-mm focal length. In spite of the long working distance of L_4 , a part of the microscope stage had to be milled out to allow for a confocal adjustment of L_4 and L_0 . In some cases, the intermediate image formed by L_4 and L_5 was further enlarged by a factor of 3 using an $f=105\ \text{mm}$, $F=2.8$ macro-objective (L_6). Thus the total magnification of the imaging system was $30\times$. The relatively large numerical aperture of the imaging system made it sensitive for the detection of plasma luminescence upon dissection or catapulting. The images were recorded by a digital camera at position 2 (FinePix S1 Pro, Fujifilm, Sendai, Japan, or Nikon D100, Nikon, Tokyo, Japan).

To be able to photograph the initial catapulting phase without vignetting by the rim of the cell chamber, we developed a special cell chamber with a removable rim. Teflon membrane and PEN foil were clamped around a flat stainless steel ring using a silicone O-ring. A flat silicone ring was placed on top of the steel ring. It was pinned down by the weight of a second stainless steel ring, and thus provided a tight seal for the culture medium. After removal of most of the culture medium shortly before LMPC, the upper steel ring and the silicone seal could also be removed, which offered an unobstructed view onto the cells on top of the PEN foil.

3 Results

3.1 Dynamics of Dissection in a Liquid Environment

The dynamics of laser-induced dissection of a cell layer on PEN foil in a liquid environment is shown in Figs. 2(a) and 2(b), and the result of the dissection process before and after catapulting is presented in Figs. 2(c) and 2(d). Culture medium had been injected between PEN and Teflon foil, and also

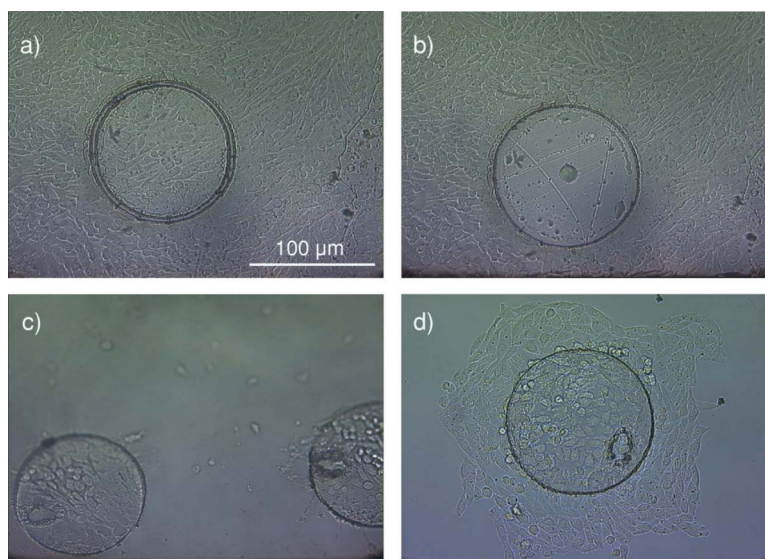


Fig. 3 Laser dissection, catapulting, and recultivation of a colony of CHO cells according to the protocol of Ref. 8. (a) After dissection, (b) after catapulting with a focused pulse, (c) catapulted specimens in the cap of a microfuge tube, and (d) after 48 h of recultivation. We used a 20 \times , NA=0.5 objective, with pulse energies of 1.0 μ J for dissection, and 12 μ J for catapulting.

covered the cells. We observed that the energy required for dissection increases in the presence of a liquid layer between Teflon membrane and PEN foil, especially when this layer is thick ($\approx 100 \mu\text{m}$). The dissection relies on plasma formation at the laser focus^{20,24} and is associated with the formation of cavitation bubbles in the culture medium [Figs. 2(a) and 2(b)]. Cells in the immediate vicinity of the cut were swept off the PEN foil by the expanding cavitation bubbles when the cell adhesion was weak. Adhesion between cells and foil was observed to decrease when cells continued to grow after forming a confluent layer. It could be improved by conditioning the foil with polylysine.

3.2 Recultivation Rates After Focused and Defocused Catapulting

LMPC and recultivation of a colony of CHO cells is demonstrated in Fig. 3. To minimize the stress on the cells, we used small pulse energies for dissection (usually 1 μJ) and catapulting (12 μJ). Furthermore, for focused catapulting, we aimed the laser at the periphery of the specimen, as visible in Figs. 3(c) and 3(d). The denuded zone at the sides of the cut is smaller than in Fig. 2, because the adhesion of the cells was better and the liquid layer between Teflon membrane and PEN foil was thinner, which facilitates dissection.

The results of catapulting with focused and defocused laser pulses are summarized in Table 2. When the laser pulse was focused into the periphery of the specimen, 16% of the catapulted specimens ($n=60$) did not arrive in the cap. Plasma formation at the rim of the specimen imparts an impulse not only in an upward but also lateral direction that results in an oblique direction of the flight trajectories. If the lateral displacement is sufficiently large, the specimens can miss the cap. Out of the specimens that could be transferred into a 12 well plate, i.e., 72% transfer rate, almost all could be recultivated, i.e., 98% or all besides one. Because we had observed that the use of a defocused laser beam for catapulting of his-

tologic specimens was associated with a stable flight trajectory, absence of hole formation, and moderate catapulting velocities when the beam diameter was comparable to the specimen diameter,¹⁶ we tested this strategy also on live cells. We used the maximum defocusing setting on the microbeam station, corresponding to a spot diameter of 50 μm . As expected, all specimens (60 out of 60) arrived in the cap, but to our surprise the majority of the cells had been sheared off the PEN foil before being captured in the microfuge cap, as shown in Figs. 4(b) and 4(c). In only four cases (7%) was recultivation possible.

3.3 Dynamics of Laser-Induced Transport

The large difference in recultivation rates after focused and defocused catapulting is not easily understood, because the geometry of membranes and liquid layers involved in live cell catapulting is complex (see Fig. 1). Therefore, we chose a stepwise approach to understand the role played by the individual layers. In the first series of experiments, dissectats of the PEN foil were catapulted from a glass slide without any liquid layers involved (Fig. 5). In a second series, a

Table 2 Rates of cells captured in the cap of a microfuge tube after catapulting with focused and defocused laser pulses of the transfer from the microfuge cap to the 12-well plate, and of the successful recultivation of the cells. The total number of specimens in each series of defocused and focused catapulting was $n=60$. Laser pulse energies used for dissection and catapulting were 1 and 12 μJ , respectively.

	Captured specimens	Transferred specimens (%)	Recultivated specimens (%)
LPC by focused pulses	84	72	98
LPC by defocused pulses	100	72	7

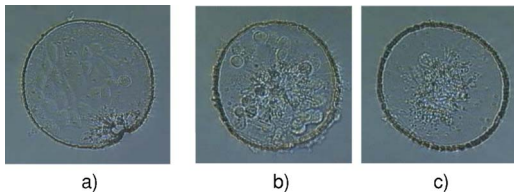


Fig. 4 Specimens with 100 μm diam after catapulting with (a) focused and (b) and (c) defocused laser pulses irradiating a spot with 50 μm diam. In (a), all cells near the specimen center remained on the PEN foil, but regions in the vicinity of the laser shot and at the opposite side of the specimen are denuded. In (b), some cells remained on the PEN foil, while the foil in (c) is completely denuded. The ablation pattern visible around the center of the specimen in (c) demonstrates that the intensity distribution in the catapulting laser beam is inhomogeneous.

30- to 50- μm -thick liquid layer was injected between underlying substrate, i.e., glass slide, and PEN foil, but no cells or liquid were present on top of the foil. The resulting dynamics are shown in Fig. 6. Finally, we investigated the catapulting dynamics of cell preparations with thin liquid layers both between Teflon and PEN foil, and above the cells (Fig. 7). Later phases of the flight dynamics, when the specimen separates from all liquid remnants, are portrayed in Fig. 8. In all experimental series, the dissectats had 100 μm diam, and we recorded one picture series using defocused laser pulses with 50- μm spot diameter and one series in which the catapulting pulses were focused at the periphery of the specimen. A description of the images and a step-by-step account of the insight gained from each picture series is given in Sec. 4.2.

4 Discussion

4.1 Laser-Induced Dissection in a Liquid Environment

Even after removal of most of the culture medium, dissection and the initial phase of catapulting still take place in a liquid environment. Thus the surrounding liquid confines the laser-produced plasma, and the ablation products cannot freely escape. As a result, a transient cavitation bubble is formed around the laser focus, as visible in Fig. 2 and discussed previously.^{20,24} This bubble expands and collapses within a few microseconds. Because of the cavitation bubble dynamics, dissection in a liquid environment is less precise than in air. For sufficiently large laser pulse energies, the shear stress exerted by the oscillating bubble causes lysis of cells adjacent to the laser focus,^{25,26} or sweeps them off the PEN foil, if their adhesion is weak. In Figs. 2(a) and 2(b), a relatively large pulse energy of $\approx 5 \mu\text{J}$ was required for dissection, because the liquid layer between the Teflon membrane and PEN foil was fairly thick. Therefore, the maximum bubble diameter amounted to $\approx 140 \mu\text{m}$. However, the width of the denuded zone on the foil is smaller; it approximately corresponds to the area in which the expanding bubble touches the cell layer. In Figs. 2(c) and 2(d), a smaller pulse energy of only $1 \mu\text{J}$ was used for dissection. Nevertheless, cells have been swept off the PEN foil by the expanding bubble up to a distance of 20 to 30 μm from the laser cut. In these experiments, the PEN membrane was not covered by polylysine, and the relatively high cell density on the foil further reduced adhesion. With optimum adhesion and small dissection energies, the damage zone next to the cut can be as narrow as 5 to 8 μm , as demonstrated in Fig. 3.



Fig. 5 Dynamics of a dry PEN foil specimen with 100 μm diam that is catapulted from a glass slide. The specimen was first completely dissected and then catapulted by a 20- μJ pulse focused through a 20 \times objective, NA=0.5, onto the rim of the specimen. The plasma luminescence indicates the location of the laser focus. The specimen performs one revolution within 2 μs , corresponding to an initial rotation frequency of 500,000 rps.

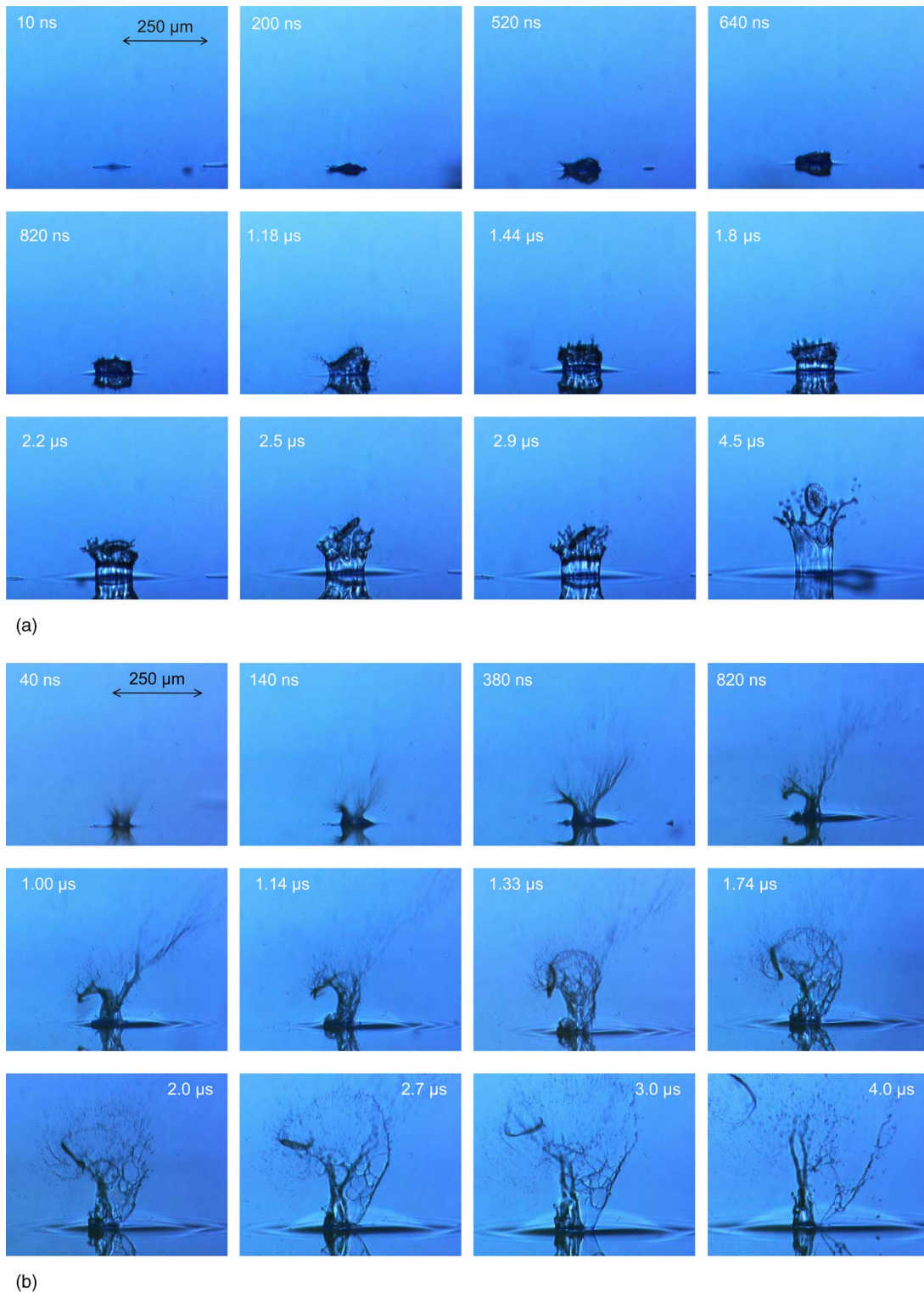


Fig. 6 Catapulting of PEN foil specimens with 100 μm diam that were located above a Teflon membrane, with a 30- to 50- μm -thick liquid layer between the two membranes. (a) Catapulting with defocused laser pulses aimed at the center of the specimen (50- μm spot diameter), and (b) catapulting with pulses focused at the periphery of the specimen. 20 \times objective, NA=0.5, and $E=20 \mu\text{J}$. The average specimen velocity during the first 4 μs is about 50 m/s in (a) and 100 m/s in (b). The rotational movement of the specimen in (b) corresponds to a frequency of $\approx 500,000$ rps during the first microsecond and 330,000 rps when averaged over the first 4 μs .



Fig. 7 Catapulting of cell preparations (CHO cells on a PEN foil that is mounted above a Teflon foil). Specimens with $100\ \mu\text{m}$ diam were catapulted out of the cell chamber after the rim had been removed. The liquid layer between Teflon and PEN foil was $30\text{-}50\ \mu\text{m}$ thick, and a $10\text{ to }50\ \mu\text{m}$ -thick layer of culture medium covered the cells. (a) Catapulting with defocused laser pulses, and (b) catapulting with pulses focused at the periphery of the specimen. $20\times$ objective, $\text{NA}=0.5$, $E=20\ \mu\text{J}$. The average specimen velocity during the first $4\ \mu\text{s}$ is about $50\ \text{m/s}$ in (a) and $55\ \text{m/s}$ in (b). The rotational movement of the specimen in (b) corresponds to a frequency of $\approx 200,000\ \text{rps}$ during the first microsecond and $125,000\ \text{rps}$ when averaged over the first $4\ \mu\text{s}$.

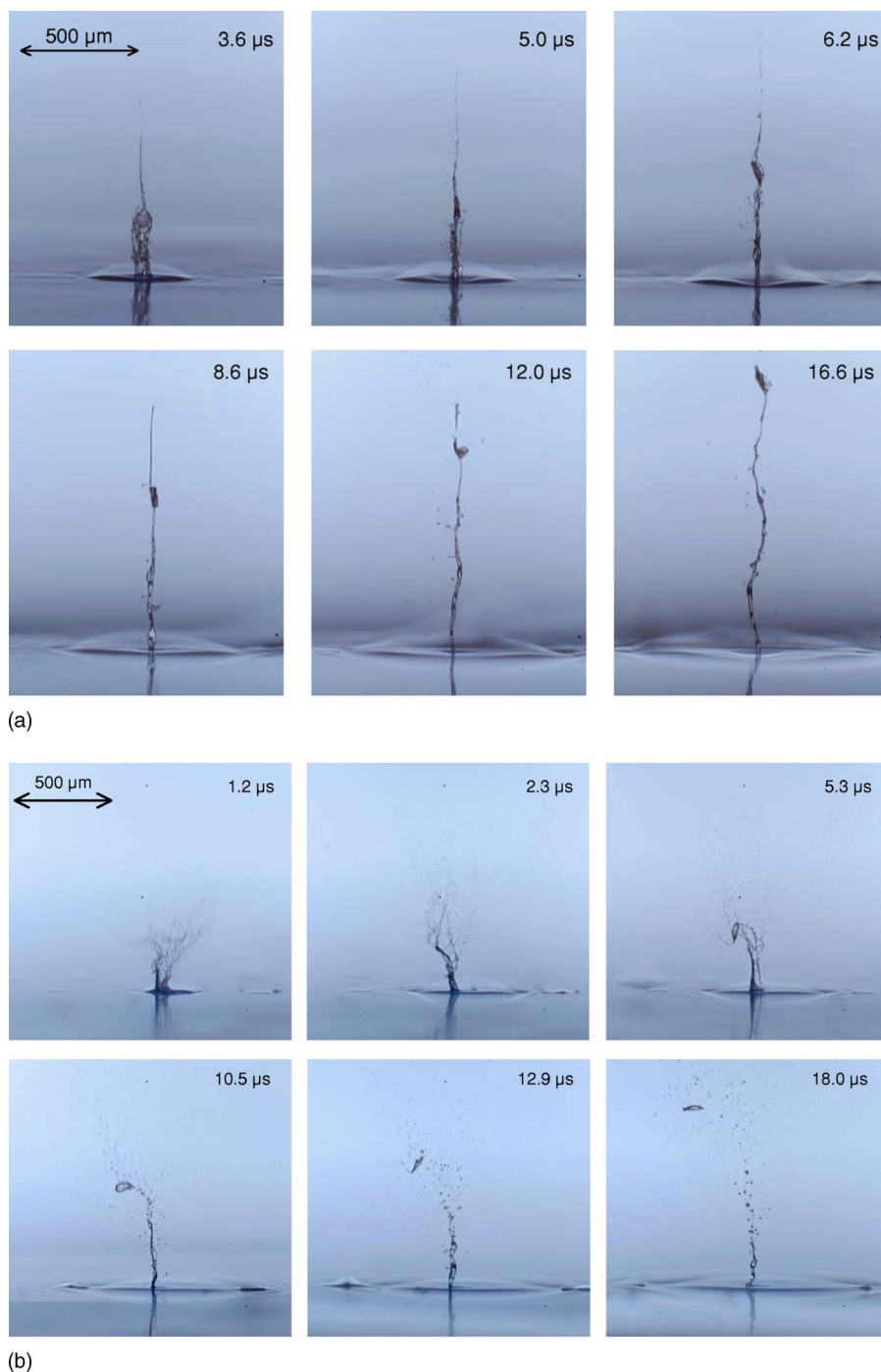


Fig. 8 Later phase of the catapulting process of cell preparations, with the same parameters as in Fig. 7. (a) Catapulting with defocused laser pulses, and (b) catapulting with pulses focused at the periphery of the specimen. The rotational movement of the specimen in (b) corresponds to a frequency of 50,000 rps when averaged over the first 20 μs . Note that the background color in this picture series differs from that in Figs. 5–7 because another digital camera with different white balance was used. (Color online only).

We employed a 20 \times objective, NA=0.5, both for dissection and catapulting, as described by Mayer et al.⁷ and Stich et al.⁸ Collateral damage during dissection could be reduced by using objectives with larger numerical apertures, because they allow for plasma-mediated cutting with smaller pulse energies that is accompanied by less pronounced cavitation effects.

4.2 Laser-Induced Transport of Live Cell Populations

The liquid layers below the PEN foil and above the cells do not only modify the dissection process but also influence the dynamics of the laser-induced transport in a complex manner. For reference, Fig. 5 shows the process in a dry environment.

A luminescent plasma is visible in all frames at the location of the laser focus. Since the laser was aimed at the rim of the specimen, the detachment is asymmetric and a strong rotational movement is introduced. After 68 ns, one half of the specimen is already detached from the substrate surface, while the other half is still attached. This results in a strong bending. When the specimen detaches from the substrate after about 400 ns, the specimen first straightens and then the bending flips over into the other direction. During the first 3 μ s, the specimen possesses an average velocity of 90 m/s in an upward direction and 10 m/s in a sideward direction, and rotates with a frequency of 500,000 rps. All these motions are soon slowed down by air friction. By comparison, when a defocused laser pulse (50- μ m spot size) is aimed under the center of the specimen, it flies straight upward with an initial velocity of 60 m/s averaged over the first 3 μ s (picture series not shown).

Figure 6 shows that the catapulting dynamics dramatically change when a liquid layer is introduced between the PEN foil and the supporting structure below this foil. In defocused catapulting [Fig. 6(a)], the expanding ablation products drive the liquid below the specimen radially to the specimen's rim, where it collides with the surrounding resting liquid. As a result, the liquid is pushed through the circular cut, and a cylindrical splash evolves. The catapulted specimen maintains a flat, disk-like shape, without bulging in the center where the laser irradiance and the ablative pressure are highest. The rim of the specimen is accelerated not only by the ablative pressure (which is lower in this region) but also by the cylindrical splash, which is driven by the ablative pressure and associated with a local concentration of kinetic energy. The combined action of ablative pressure and secondary fluid flow results in an approximately homogeneous acceleration of the sample, which thus maintains a flat shape.

By contrast, in focused catapulting [Fig. 6(b)], the side of the specimen at which the laser focus is located is most strongly accelerated, and the specimen assumes a fast rotational movement. Within $\approx 2.7 \mu$ s, it has turned by 360 deg, corresponding to a rotation frequency of 370,000 rps, which is not much slower than for the case of catapulting from a dry substrate shown in Fig. 5. The catapulting velocity is larger than with defocused pulses ($v \approx 80$ m/s averaged over the first 2 μ s compared to $v \approx 45$ m/s), because plasma is formed at the laser focus, while defocused catapulting is driven by ablation below the threshold for plasma formation.

So far, the dynamics in Fig. 6 show no obvious advantage of focused catapulting for live cell retrieval and recultivation, as given in Table 2. This advantage arises only when PEN foils and cells are covered with a liquid layer such as in Fig. 7 (early phase) and Fig. 8 (later phase). For defocused catapulting, the upper liquid layer now largely suppresses the splash of liquid from the lower layer, and the specimen is hardly accelerated at its periphery. The high pressure produced by ablation in the central region of the specimen results in an upward bulging of this region, while the rim is tied down by the inertia of the liquid covering the specimen [Fig. 7(a)]. After about one microsecond, the movement of the specimen center is slowed down by these inertial forces, while the radial liquid flow in the upper liquid layer that was created during the first microsecond continues and is focused above

the specimen center into an upward directed jet. Because this jet flow is faster than the movement of the specimen, it exerts a shear force on the cells. When the specimen rises out of the liquid, after a few microseconds, some fluid stays behind at the specimen's rim. This results in flow and shear forces opposite that of the jet flow. Even after 16.5 μ s, the specimen is not yet completely freed from the culture medium [Fig. 8(a)]. The combined action of the successive shear forces is probably responsible for the removal of most of the cells from the specimen that led to the low success rate of recultivation.

The catapulting dynamics induced by laser pulses focused at the periphery of the dissectat are presented in Fig. 7(b). Its principal characteristics resemble the sequence of events observed without a liquid layer covering the cells [Fig. 6(b)]. The pressure within the laser plasma is strong enough to immediately remove the upper liquid layer in the vicinity of the laser focus. This "Moses effect" gives leeway to the acceleration of the side of the specimen proximal to the laser focus. Within about one microsecond, the specimen has risen out of the culture medium and rotated by 90 deg, and after about 4 μ s, it has propagated a distance of 220 μ m (average velocity 55 m/s) and rotated by 180 deg (rotation frequency 125,000 rps). Because of the rotation, the fluid flow along the cells during the specimen's take off remains weak, and the shear forces acting on the cells are weaker than in the case of defocused catapulting. On the other hand, centrifugal forces come into play that increase proportional to the distance r from the axis of rotation. After 5 to 20 μ s [Fig. 8(b)], the specimen flies free of any liquid, and the rotational movement has been considerably slowed down to 50,000 rps by air friction.

Both for focused and defocused catapulting, the exact sequence of events varies with the thickness of the liquid layer above the cells (10 to 50 μ m) but still resembles the behavior portrayed in Figs. 7 and 8. After removal of the culture medium, the liquid layer thins because of evaporation. The actual thickness on each individual photograph thus depends on the time after removal of the medium when catapulting was performed. The main consequence of an increasing layer thickness are a slow down of the translational and rotational specimen velocities, and an increase of the fluid reservoir capable of inducing shearing forces on the cells.

4.3 Possible Side Effects and Their Minimization

During the *dissection* step, some cells are already lost for catapulting and recultivation because they are sheared off the PEN foil (Fig. 2). A first approach to reduce this collateral damage during dissection can be using objectives with larger numerical aperture, because they allow for plasma-mediated cutting with smaller pulse energies. Furthermore, finer dissections than possible with the N₂ laser employed in our experiments can be achieved by an improvement of the beam profile, and by a reduction of the laser pulse duration in combination with an increase of the laser repetition rate. The beam profile of diode-pumped frequency-tripled Nd:YAG lasers that are incorporated in the newest generation of most commercial microbeam system is much better than that of the N₂ laser. This can lead to a considerable reduction of the focal spot size, optical breakdown energy, and cutting width, provided that the delivery optics to the focusing microscope ob-

jective maintain good beam quality. An even larger reduction of the energy threshold for optical breakdown can be reached by employing shorter laser pulse durations.^{27,28} We observed that a reduction of the pulse duration from 6 ns to 300 fs reduces the breakdown threshold at NA=0.9 by a factor of approximately 100 for UV wavelengths and even more for IR wavelengths (unpublished results). When very small single pulse energies are used for dissection, a large number of pulses is necessary to complete a cut of finite length. Therefore, the repetition rate of the laser pulses must be sufficiently large (≥ 1 kHz) to avoid an impractical prolongation of the processing time.

General criteria for successful live cell *catapulting* are: 1. the fraction of specimens that can be recovered/collected, 2. the percentage of vital cells per specimen, and 3. the recultivation rate. Adverse factors are: 1. large variations in the flight trajectories of the specimens, 2. removal of cells from the substrate by mechanical forces, and 3. damage to cells remaining on the substrate by heat, UV irradiation, or mechanical stress. While the flight trajectories were more stable with defocused catapulting, cell loss and damage were less severe when pulses focused at the rim of the specimen were used. We see later that these differences are probably due to distinctions in the mechanical effects, rather than to dissimilar responses to heat and UV irradiation.

Possible sources for cellular damage by heat and UV radiation are similar to those for histologic material that were discussed in detail in a previous publication.¹⁶ Using the comet assay, the threshold for photochemical DNA damage was found to be 1.5 J/cm^2 for $\lambda=340 \text{ nm}$.²⁹ Because of the limited sensitivity of the comet assay, approximately 300 strand breaks per cell are necessary to detect DNA damage. Hence, one single DNA strand break per cell is expected to occur after a radiant exposure of 5 mJ/cm^2 . For broadband radiation (305 to 350 nm) peaking at 325 nm, significant cell killing was observed with light doses $\geq 1 \text{ J/cm}^2$.³⁰

For defocused catapulting at $50\text{-}\mu\text{m}$ spot size and $12\text{-}\mu\text{J}$ pulse energy, such as used in the recultivation study, the radiant exposure incident on the PEN foil is 0.6 J/cm^2 and the dose transmitted through the foil that reaches the cells is 0.12 J/cm^2 . This value is well below the damage threshold detectable with the comet assay and below the threshold for significant cell killing, but higher than the estimated value for single-strand breakage. Potential hazards may be reduced by using larger spot sizes and smaller laser pulse energies. To achieve reproducible catapulting with small pulse energies, the liquid layer above the cells must be very thin and its thickness controlled, as discussed in Sec. 5.

By contrast, when focused laser pulses are used for catapulting, the cells in the immediate vicinity of the focus are not only damaged by UV irradiation, but directly disintegrated by the high temperatures and strong mechanical forces originating from the plasma. However, more than 97% of the specimen is not at all affected by UV radiation, because only a small part of the sample is irradiated by the laser light.

The thresholds for thermal cell damage are high for the short heat exposure times involved in catapulting, which last only a few microseconds.^{16,23} Simanowski et al.²² reported that cells survived temperatures as high as 180°C for heat exposure time of $300 \mu\text{s}$. For heat pulses shorter than

$300 \mu\text{s}$, the threshold for cellular death was determined by the threshold for explosive vaporization that occurred at temperatures slightly above 200°C . When defocused pulses are used for catapulting, cells are not exposed to such high temperatures, because the PEN foil serves as a thermal shield. With focused pulses, such temperatures are easily exceeded in the immediate vicinity of the laser plasma, but only a tiny fraction of the specimen is affected.

Thus, the most likely sources of cell damage in catapulting are the mechanical effects that are associated with fast acceleration out of the culture medium. They may result in removal of cells from the membrane, immediate cell lysis, or in more subtle damage to cell membranes and/or organelles.

Looking at the vigorous dynamics portrayed in Figs. 7 and 8, it is quite remarkable that a large number of catapulted cells continue to proliferate in an apparently unimpeded fashion. However, it needs to be kept in mind that rapid motions per se do not necessarily cause damage. Any fluid motion can be decomposed in uniform translation, rigid rotation, and an extensional flow, and only the latter bears damage potential. Extensional flow patterns associated with tensile stress arise from shear through pressure gradients, inertial or viscous drag, from radial expansion movements,^{31,32} or from thermoelastic effects.^{20,33} When the spot size irradiated by a defocused laser pulse ($50 \mu\text{m}$ in our experiments) is considerably smaller than the specimen diameter ($100 \mu\text{m}$ in our experiments), the initial pressure distribution is inhomogeneous, and the center of the specimen will bulge upward before it flies off, due to the expansion of the bubble below the specimen. The resulting tensile stress and strain may lead to cell detachment or membrane rupture. For later phases of the catapulting dynamics, the image series in Figs. 7 and 8 suggest that shear forces are also more pronounced in catapulting with a defocused rather than a focused laser beam.

However, catapulting with pulses focused at the specimen's rim is associated with a fast rotation of the specimens that gives rise to considerable centrifugal forces that are not observed in defocused catapulting. The initial rotational velocity at the rim of a specimen with $100 \mu\text{m}$ diam revolving by 180 deg in $4 \mu\text{s}$, such as in Fig. 7(b), is $\approx 39 \text{ m/s}$, and the centripetal acceleration $a=v^2/r$ at the specimen rim ($r=50 \mu\text{m}$) amounts to $3 \times 10^7 \text{ m/s}^2$ for $\nu=125,000 \text{ rps}$. Correspondingly, cells far away from the rotation axis are sheared off—not only in the vicinity of the laser shot but also at the opposite side of the specimen rim as visible in Fig. 4(a). Nevertheless, the majority of the cells remain on the specimen in spite of the strong centrifugal forces, possibly due to their relatively short duration. Air friction rapidly decelerates the rotational movement, and correspondingly the centrifugal force $F=mv^2/r$ drops very fast, such that strong centrifugal forces act only during a few microseconds. This time interval is apparently short enough to allow for elastic deformation, avoiding rupture or detachment of cells that are located sufficiently close to the rotation axis. Note, however, that the shear forces associated with the tangential flow in defocused catapulting act only about five times longer than the strong centrifugal forces arising when laser pulses are focused at the rim of the specimen. It is not yet fully understood how this relatively small difference is linked to the observed large disparity in cell attachment.

In general, the damage potential of hydrodynamic effects is not only determined by the magnitude of the tensile or shear forces, but also by their duration, because the material must be strained before it can rupture. Rupture (or at least poration) of the cell membrane requires an areal strain larger than 2 to 3%.^{34–36} The deforming force must last sufficiently long to achieve this deformation. Moreover, the ultimate tensile strength (UTS) of the cell membrane or elements of the cytoskeleton may depend on the strain rate. It has been observed for tissue that, while the strain at fracture does not change significantly with strain rate, the UTS increases. The increase of the UTS is due to the fact that, under conditions of rapid deformation, there is significant viscous dissipation between matrix elements, for example collagen fibrils, and ground substance.²⁰ It is conceivable that similar laws also apply on the cellular level. The response of cells to very large strain rates acting for very short times is still largely unexplored and requires further investigation.

5 Conclusions and Outlook

Due to the large number of layers involved in the present technique, many parameters determine the catapulting dynamics. Among those, the laser spot size, the laser energy, and the thickness of both liquid layers (below the PEN foil and above the cells) are especially important. We observed that a thin liquid layer between Teflon membrane and PEN foil facilitates catapulting. However, it increases the energy requirements for cutting and thus the amount of side effects associated with dissection when it becomes too thick. The optimum thickness of this layer, which may vary with specimen size, still needs to be identified. The thickness of the liquid layer above the cells is even more important. In the present study, it varied between 10 and 50 μm , and catapulting with laser pulses focused at the sample periphery yielded considerably better results for the separation and recultivation of live cells than the use of defocused pulses with 50- μm spot size that were aimed at the specimen center. Improvements of defocused catapulting can probably be achieved with stronger defocusing and a more homogeneous irradiance distribution at the specimen than in our present experiments, which would reduce bulging of the sample. However, even under those conditions the advantage of the rotational movement associated with focused catapulting may still prevail if the liquid layer above the cells is too thick. A way out might be the use of defocused laser pulses aimed at a locus between the sample center and periphery. Depending on the degree of decentration, one could adjust the rotational movement such that shearing and centrifugal forces are minimized.

For gentle and reproducible catapulting, the thickness of the liquid layer above the cells should generally be as small as possible without risking desiccation of the cells, regardless of whether focused or defocused pulses are used. In our experiments, in which the thickness of the liquid layer varied between 10 and 50 μm , the laser pulse energy had to be sufficiently large to overcome the resistance of a 50- μm -thick layer to achieve reliable catapulting. A thinner layer with reproducible thickness would provide a well-defined catapulting threshold and enable the use of smaller laser pulse energies close to this threshold, which would then result in minimum flight velocities, shearing forces, and centrifugal forces. This

goal can possibly be achieved by overlaying a very thin layer of mineral oil on top of the culture medium shortly before the majority of culture medium is removed to prepare for catapulting. A film just a few nanometers thick would already stabilize the thickness of the remaining culture medium by reducing evaporation losses. For control of the layer thickness until a preset endpoint is reached during removal of the culture medium, it could be monitored by means of optical coherence tomography.³⁷ If it becomes possible to control and minimize the thickness of the culture medium film above cells, a catapulting dynamic similar to that shown in Fig. 8(a) may be achieved when defocused laser pulses are used for catapulting. In this case, it might become feasible to extract very small groups of cells or even single cells, similar to histologic catapulting. This goal is not achievable when tightly focused laser pulses are used for catapulting, because in that case, the cells in the immediate vicinity of the laser focus are likely to be destroyed.

Acknowledgments

This work was sponsored by the German Bundesministerium für Bildung und Forschung (BMBF) under grant number 13N8461. Palm Microlaser Technologies provided the microbeam system used. We appreciate stimulating discussions with Karin Schütze, Bernd Sägmüller, and Yilmaz Niyaz of Palm-Microlaser Technologies, and with Heyke Diddens (Institute of Biomedical Optics, University of Lübeck), who also provided the CHO cell line used for live cell catapulting. The suggestion to use oil to prevent evaporation of the culture medium shortly before catapulting was made by one of the reviewers of this work. We thank Sebastian Freidank, Florian Wölbeling, Helge Meyer, and Reinhard Schulz of the Institute of Biomedical Optics, University of Lübeck, for technical assistance.

References

1. I. A. Eltoun, G. P. Siegal, and A. R. Frost, "Microdissection of histologic sections: past, present, and future," *Adv. Anat. Pathol.* **9**, 316–322 (2002).
2. J. Kehr, "Single cell technology," *Curr. Opin. Plant Biol.* **6**, 617–621 (2003).
3. S. Thalhammer, G. Lahr, A. Clement-Sengewald, W. M. Heckl, R. Burgemeister, and K. Schütze, "Laser microtools in cell biology and molecular medicine," *Laser Phys.* **13**, 681–691 (2003).
4. K. Schütze and G. Lahr, "Identification of expressed genes by laser-mediated manipulation of single cells," *Nat. Biotechnol.* **16**, 737–742 (1998).
5. K. Schütze, H. Pösl, and G. Lahr, "Laser micromanipulation systems as universal tools in molecular biology and medicine," *Cell Mol. Biol. (Paris)* **44**, 735–746 (1998).
6. G. Lahr, "RT-PCR from archival single cells is a suitable method to analyze specific gene expression," *Lab. Invest.* **80**, 1477–1479 (2000).
7. A. Mayer, M. Stich, D. Brocksch, K. Schütze, and G. Lahr, "Going in vivo with laser microdissection," *Methods Enzymol.* **356**, 25–33 (2002).
8. M. Stich, S. Thalhammer, R. Burgemeister, G. Friedemann, S. Ehnle, C. Lüthy, and K. Schütze, "Live cell catapulting and recultivation," *Pathol. Res. Pract.* **199**, 405–409 (2003).
9. R. Burgemeister, "New aspects of laser microdissection in research and routine," *J. Histochem. Cytochem.* **53**, 409–412 (2005).
10. S. Langer, J. B. Giegl, S. Ehnle, R. Gangnus, and M. R. Speicher, "Live cell catapulting and recultivation does not change the karyotype of HCT116 tumor cells," *Cancer Genet. Cytogenet.* **161**, 174–177 (2005).
11. P. K. Wu, B. R. Ringeisen, D. B. Krizman, C. G. Fronzoza,

- M. Brooks, D. M. Bubb, R. C. Y. Auyeung, A. Piqué, B. Spargo, R. A. McGill, and D. B. Chrisey, "Laser transfer of biomaterials: matrix-assisted pulsed laser evaporation (MAPLE) and MAPLE Direct Write," *Rev. Sci. Instrum.* **74**, 2546–2557 (2006).
12. B. R. Ringeisen, H. Kim, J. A. Barron, D. B. Krizman, D. B. Chrisey, S. Jackman, R. Y. C. Auyeung, and B. J. Spargo, "Laser printing of pluripotent embryonal carcinoma cells," *Tissue Eng.* **10**, 483–491 (2004).
 13. J. A. Barron, P. Wu, H. D. Ladouceur, and B. R. Ringeisen, "Biological laser printing: a novel technique for creating heterogeneous 3-dimensional cell patterns," *Biomed. Microdevices* **6**, 139–147 (2004).
 14. B. Hopp, T. Smausz, N. Kresz, N. Barna, Z. Bor, L. Kolozsvari, D. B. Chrisey, A. Szabo, and A. Nogradi, "Survival and proliferative ability of various living cell types after laser-induced forward transfer," *Tissue Eng.* **11**, 1817–1823 (2005).
 15. B. Hopp, T. Smausz, N. Barna, C. Vass, Z. Antal, L. Kredics, and D. B. Chrisey, "Time-resolved study of absorbing film assisted laser induced forward transfer of *Trichoderma longibrachiatum* conidia," *J. Phys. D* **38**, 833–837 (2005).
 16. A. Vogel, K. Lorenz, V. Horneffer, G. Huettmann, D. von Smolinski, and A. Gebert, "Mechanisms of laser-induced dissection and transport of histologic specimens," *Biophys. J.* **93**(12) (2007).
 17. R. A. J. Litjens, T. I. Quickenden, and C. G. Freeman, "Visible and near-ultraviolet absorption spectrum of liquid water," *Appl. Opt.* **38**, 1216–1223 (1999).
 18. H. Kuchling, *Taschenbuch der Physik*, Carl Hanser Verlag, München, Wien (1991).
 19. See <http://www.m-petfilm.com>.
 20. A. Vogel and V. Venugopalan, "Mechanisms of pulsed laser ablation of biological tissues," *Chem. Rev. (Washington, D.C.)* **103**, 577–644 (2003).
 21. J. Neumann and R. Brinkmann, "Boiling nucleation on melanosomes and microbeads transiently heated by nanosecond and microsecond laser pulses," *J. Biomed. Opt.* **10**, 024001 (2005).
 22. D. Simanowski, M. Sarkar, A. Irani, C. O'Connell-Rodwell, C. Contag, A. Schwettman, and D. Palanker, "Cellular tolerance to pulsed heating," *Proc. SPIE* **5695**, 254–259 (2005).
 23. D. M. Simanowskii, M. A. Mackanos, A. R. Irani, C. E. O'Connell-Rodwell, C. H. Contag, H. A. Schwettman, and D. V. Palanker, "Cellular tolerance to pulsed hyperthermia," *Phys. Rev. E* **74**, 011915 (2005).
 24. V. Venugopalan, A. Guerra, K. Nahen, and A. Vogel, "The role of laser-induced plasma formation in pulsed cellular microsurgery and micromanipulation," *Phys. Rev. Lett.* **88**, 078103 (2002).
 25. K. R. Rau, A. Guerra, A. Vogel, and V. Venugopalan, "Investigation of laser-induced cell lysis using time-resolved imaging," *Appl. Phys. Lett.* **84**, 2940–2942 (2004).
 26. K. R. Rau, P. A. Quinto-Su, A. N. Hellman, and V. Venugopalan, "Pulsed laser microbeam-induced cell lysis: time-resolved imaging and analysis of hydrodynamic effects," *Biophys. J.* **91**, 317–329 (2006).
 27. A. Vogel, K. Nahen, and D. Theisen, "Plasma formation in water by picosecond and nanosecond Nd:YAG laser pulses—Part I: optical breakdown at threshold and superthreshold irradiance," *IEEE J. Sel. Top. Quantum Electron.* **2**, 847–860 (1996).
 28. A. Vogel, J. Noack, G. Hüttmann, and G. Paltauf, "Mechanisms of femtosecond laser nanosurgery of cells and tissues," *Appl. Phys. B* **81**, 1015–1047 (2005).
 29. A. de With and K. O. Greulich, "Wavelength dependence of laser-induced DANN damage in lymphocytes observed by single-cell gel electrophoresis," *J. Photochem. Photobiol., B* **30**, 71–76 (1995).
 30. D. Bertling, F. Lin, and A. W. Girotti, "Role of hydrogen peroxide in the cytotoxic effects of UVA/B radiation on mammalian cells," *Photochem. Photobiol.* **64**, 137–142 (1996).
 31. M. Lokhandwalla and B. Sturtevant, "Mechanical haemolysis in shock wave lithotripsy (SWL): I. analysis of cell deformation due to SWL flow-fields," *Phys. Med. Biol.* **46**, 413–437 (2001).
 32. M. Lokhandwalla, J. A. McAteer, J. C. Williams, Jr., and B. Sturtevant, "Mechanical haemolysis in shock wave lithotripsy (SWL): II. In vitro cell lysis due to shear," *Phys. Med. Biol.* **46**, 1245–1264 (2001).
 33. G. Paltauf and P. Dyer, "Photomechanical processes and effects in ablation," *Chem. Rev. (Washington, D.C.)* **103**, 487–518 (2003).
 34. E. A. Evans, R. Waugh, and L. Melnik, "Elastic area compressibility modulus of red cell membrane," *Biophys. J.* **16**, 585–595 (1976).
 35. D. Needham and R. S. Nunn, "Elastic deformation and failure of liquid bilayer membranes containing cholesterol," *Biophys. J.* **58**, 997–1009 (1990).
 36. D. Boal, *Mechanics of the Cell*, Cambridge Univ. Press, Cambridge, UK (2002).
 37. A. Fercher, W. Drexler, C. K. Hitzenberger, and T. Lasser, "Optical coherence tomography—principles and applications," *Rev. Roum. Phys.* **66**, 239–303 (2003).